Optics Letters

Single-shot photofragment imaging by structured illumination

KAJSA LARSSON,* MALIN JONSSON, JESPER BORGGREN, ELIAS KRISTENSSON, ANDREAS EHN, MARCUS ALDÉN, AND JOAKIM BOOD

Division of Combustion Physics, Department of Physics, Lund University, P.O. Box 118, 221 00 Lund, Sweden
**Corresponding author: Kajsa.Larsson@forbrf.lth.se*

Received 25 August 2015; revised 25 September 2015; accepted 5 October 2015; posted 6 October 2015 (Doc. ID 248657); published 26 October 2015

A laser method to suppress background interferences in pump–probe measurements is presented and demonstrated. The method is based on structured illumination, where the intensity profile of the pump beam is spatially modulated to make its induced photofragment signal distinguishable from that created solely by the probe beam. A spatial lock-in algorithm is then applied on the acquired data, extracting only those image components that are characterized by the encoded structure. The concept is demonstrated for imaging of OH photofragments in a laminar methane/air flame, where the signal from the OH photofragments produced by the pump beam is spatially overlapping with that from the naturally present OH radicals. The purpose was to perform for the first time, to the best of our knowledge, single-shot imaging of HO_2 in a flame. These results show an increase in signal-to-interference ratio of about 20 for single-shot data.

OCIS codes: (300.6360) Spectroscopy, laser; (280.1740) Combustion diagnostics; (280.2470) Flames; (300.2530) Fluorescence, laser-induced.

http://dx.doi.org/10.1364/OL.40.005019

Pump–probe laser techniques are widely applied in ultrafast spectroscopy [1,2]; for example, nonequilibrium molecular dynamics may be investigated by transient terahertz spectroscopy [3] or femtosecond transition–state spectroscopy [4]. In general, the pump pulse modifies a sample whereupon a probe pulse senses the modification at a certain time delay. The sample modification, for example, could be the production of a molecular fragment (photofragment), whose presence is sensed by a probe laser. Photofragmentation followed by fragment detection is commonly used in chemical analysis; for an extensive review, see [5,6] and references therein. A significant difficulty arises if the fragment species is naturally present, as this will generate a spectrally identical background signal, i.e., the probe laser senses both the photofragment and the naturally existing fragment species. Subtraction of a signal recorded without launching the pump pulse, i.e., the background contribution, is a possible solution for stationary samples, but requires that the signal difference caused by variation in the probe laser intensity between the two measurements is significantly less than the photofragment signal. Thus, the lower the signal-to-background ratio, the higher the demand on the probe laser and sample stability.

Laser-induced fluorescence (LIF) is a sensitive technique for imaging of trace species distributions. There are, however, numerous species that lack bound excited electronic states, which prevents imaging with LIF using UV/visible excitation. Such molecules may be visualized using a technique called photofragmentation laser-induced fluorescence (PFLIF), which is a pump–probe technique originally proposed by Rodgers *et al.* [7]. In PFLIF, a pump pulse photodissociates a parent molecule, whereupon a probe pulse tuned to an absorption line of the created photofragment induces fluorescence whose intensity is related to the concentration of the parent molecule [8]. Photofragmentation laser-induced fluorescence, for example, can be used for imaging of hydrogen peroxides in flames [9]. Here, the pump laser photodissociates the hydrogen peroxides into OH photofragments, which are detected with a probe pulse that induces fluorescence from the OH photofragments. This application represents an excellent example of a measurement situation in which the aforementioned issue with a strong background signal is particularly difficult, as fluorescence from naturally present OH radicals is induced by the probe laser. Traditionally, two images have to be acquired, with and without the pump pulse fired [9], and the signal difference between the two images determines the photofragment signal from the hydrogen peroxides. As already alluded to, this method is very sensitive to fluctuations in laser pulse energy between the two image recordings and is not capable of delivering single-shot images, which is an absolute requirement for studies in nonstationary environments.

Structured illumination (SI) is a method used primarily for microscopic imaging, where it is employed to remove out-of-focus intensity contributions [10]. With SI, a fringe pattern is projected onto the sample of interest to mark the in-focus plane, making it distinguishable from other layers. By altering the spatial phase of this superimposed line structure and recording three so-called subimages, out-of-focus light can be rejected

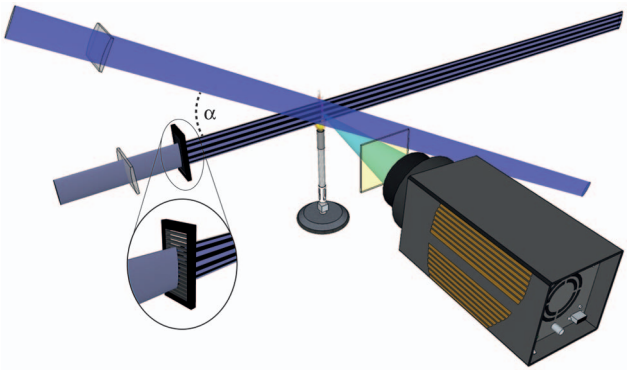

Fig. 1. Schematic of the experimental setup. The pump beam is guided through a metallic grating that adds the required modulation structure to its intensity profile. The crossing angle, α, is the vertical angle between the pump pulse and the probe pulse in relation to the pump pulse.

in the post-processing of the data. Berrocal *et al.* have demonstrated a planar configuration of SI that offers improved visualization of turbid spray systems [11] and was later combined with a spatial frequency lock-in methodology to permit single-shot imaging [12]. Using a spatial frequency lock-in method in the post-processing routine allows for removal of unwanted signals with different spatial frequencies than those in the frequency-encoded sheet, such as multiply scattered light or background stray light.

In this Letter, PFLIF is combined with SI, and the data are analyzed using a spatial frequency lock-in algorithm. The algorithm is based on the procedure presented in [12], but the current approach has additional steps that improve its overall sensitivity, permitting weaker signals to be detected. Single-shot PFLIF imaging of OH photofragments generated from mainly the hydroperoxyl radical (HO_2) [9] in a laminar methane (CH_4)/air flame is presented. This application exemplifies how a weak signal can be extracted from a significantly stronger background, in this case, stemming from the naturally present OH radicals in the flame—a long-standing challenge in the field of combustion diagnostic research.

The experimental setup is a combination between an optical arrangement for PFLIF and SI; see [9] for details of a general PFLIF experimental setup. Below is a brief description of the current system. A schematic of the experimental setup is depicted in Fig. 1. The fourth harmonic (266 nm) from an Nd:YAG laser was used as a pump pulse. To incorporate SI, the intensity profile of the 266 nm beam was spatially modulated using a metal grating with a line separation of 0.3 mm. Naturally present OH radicals and OH photofragments were probed by an Nd:YAG pumped dye laser roughly 100 ns after the pump pulse. This pump–probe delay time is sufficiently long for the OH photofragments to be in thermal equilibrium and short enough to prevent any significant chemical interference in the flame [9]. The probe pulse had a wavelength of 281.91 nm, corresponding to the overlapping $Q_1(1)$ and $R_2(3)$ transition of the $A^2\Sigma^+(v=1) \leftarrow X^2\Pi(v=0)$ absorption band of OH. Spatial filtering was used on the probe pulse to smooth the beam profile and suppress spatial frequencies that potentially could interfere with the modulated signal. Both laser systems are pulsed with a repetition rate of 10 Hz and pulse durations of 5–10 ns. Both the pump and probe beams were shaped into laser sheets by two separate lens configurations and overlapped in such a way that the measurement volume was limited to the reaction and unburned zones of the flame. The overlap of the laser beams had a crossing angle, which reduces the risk of signal crosstalk between the frequency-coded fluorescence and irregularities in the probe–beam profile that matches the modulation frequency of the pump beam. Such irregularities, if present, will thus appear with a different angle and, thereby, reside at a different location in the Fourier domain and are filtered out by the lock-in algorithm.

The laser fluence of the pump and probe sheets was 4.2 J/cm^2 and 0.03 J/cm^2, respectively. Both of these fluences are low enough to keep from causing saturation of either the photolysis or the OH fluorescence.

The OH photofragment signal was imaged with an intensified CCD camera equipped with a UV-objective and spectrally filtered with a Schott WG305 filter in front of the camera lens. The experiments were carried out in a laminar Bunsen-type CH_4/air flame at stoichiometric conditions.

To demonstrate the spatial frequency lock-in routine, an accumulated intensity modulated PFLIF image, I_{RAW}, of a CH_4/air flame is presented in Fig. 2(a). The majority of the signal proceeds from naturally present OH radicals, and virtually no modulation signal from the OH photofragments stemming from mainly HO_2 is observed in the reaction zone of the flame. In the evaluation routine, a circular Gaussian window is first applied to the image to remove sharp edges that otherwise produce image artifacts in the image post-processing routine. Second, I_{RAW} is transformed to the Fourier plane, $\mathcal{F}(I_{RAW})$, and presented in Fig. 2(b), where the first harmonic of the modulated signal is seen on both sides of the origin surrounded by white ellipses. Here, both structural frequencies caused by the discrete pixel architecture of the camera and the probe laser beam profile are clearly seen as they are crossing the origin. The crossing angle, α, is indicated in the Fourier plane. As a third step, unwanted background interferences are extracted by applying an inverted band-pass filter on $\mathcal{F}(I_{RAW})$ that suppresses the modulation frequency. The white ellipses in Fig. 2(b) show these elliptical band-pass filters in the Fourier domain. Inverse Fourier transforming this modified $\mathcal{F}(I_{RAW})$ will result in an image only containing the background information, I_{BKG}; see Fig. 2(c). A self-compensated image, I_{SC}, is generated as a fourth step by taking the ratio between I_{RAW} and I_{BKG}; here, the strong background interferences are reduced, and the modulated signal is enhanced [see Fig. 2(d)]. Dividing I_{RAW} with I_{BKG} is reminiscent of compensating for the probe laser beam profile. As a fifth step, I_{SC} is Fourier transformed, $\mathcal{F}(I_{SC})$, and presented in Fig. 2(e); here, it is clearly seen that most of the unwanted interfering background signals from Fig. 2(b) are removed.

To extract the intensity modulated signal and remove any remaining traces of background interferences, a band-pass filter generated as an elliptical super Gaussian window orientated at the desired fundamental spatial frequency, is multiplied with $\mathcal{F}(I_{SC})$. The white ellipse in Fig. 2(e) shows this elliptical band-pass filter in the Fourier domain. As a final step, the band-pass filtered signal is frequency shifted to the origin and inversely Fourier transformed; the final image, I_{PFLIF}, is extracted as the absolute value and depicted in Fig. 2(f). It should be emphasized that all the images are extracted from I_{RAW}.

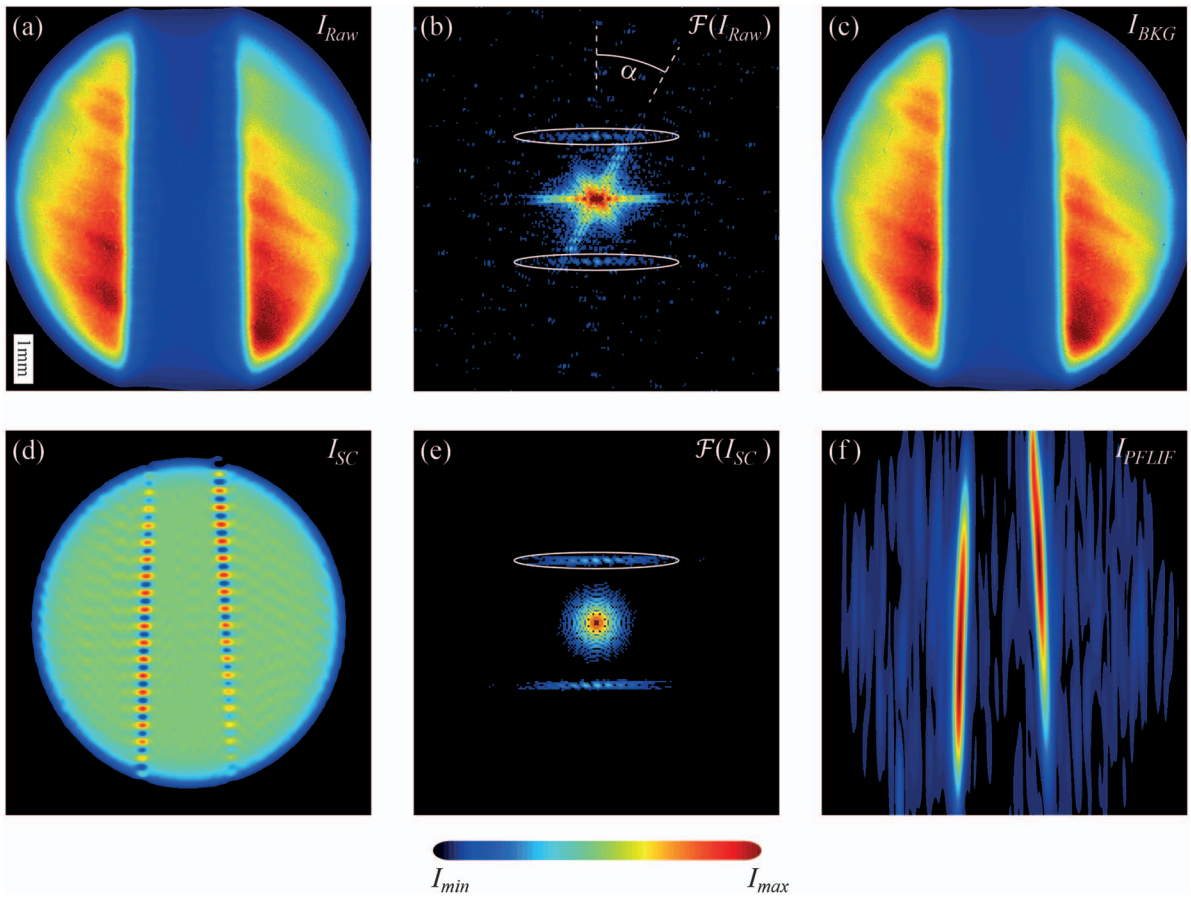

Fig. 2. (a) I_{RAW}, an average PFLIF image. The scale bar indicates 1 mm. The pump beam propagates horizontally through the flame from the left part of the image, while the probe beam propagates through the flame from a crossing angle, α, starting from the upper-left corner of the image. The burner is oriented so that the unburned zone is the blue part in the center of the image; see Fig. 1 for details. (b) $\mathcal{F}(I_{\mathrm{RAW}})$, the Fourier transformation of I_{RAW} showing the first harmonic of the modulated signal on both sides of the origin. The white ellipses show the super Gaussian band-pass filter around the modulated OH photofragment signal. The crossing angle, α, is indicated in the Fourier plane. (c) I_{BKG}, background extracted from I_{RAW}. (d) I_{SC}, OH photofragment signal of the ratio between I_{RAW} and I_{BKG}. (e) (I_{SC}), the Fourier transformation of I_{SC} showing the first harmonic of the modulated signal on both sides of the origin. The white ellipse shows the super Gaussian band-pass filter around the modulated OH photofragment signal. (f) I_{PFLIF}, the OH photofragment signal stemming from mainly HO_2.

The frequency of the modulation will determine the distance between the fundamental frequency component and the origin in the Fourier plane. With a higher modulation frequency, more spatial frequencies can be preserved. Figure 3(a) shows a single-shot image, I_{RAW}, recorded by PFLIF with an intensity modulated pump–laser sheet in a CH_4/air flame. The circular shape of the image is once again due to the circular Gaussian window that was applied to remove sharp edges of the image. Figure 3(b) presents I_{PFLIF}, containing an extracted signal from I_{RAW}. This extracted signal is from OH photofragments stemming mainly from HO_2. To show the statistical significance of the detected signal, a 2 mm vertical cross section of 300 single-shot images of I_{PFLIF} were analyzed. The mean signal is shown as the thick blue line in Fig. 3(c), while the standard deviation is shown as the gray region around the blue line. A 2 mm vertical cross section of 300 single-shot images of I_{RAW} is presented as the red line in Fig. 3(c). In Fig. 3(d), the 2 mm vertical cross section of I_{PFLIF} is shown as the blue line, while a 2 mm vertical cross section of I_{RAW} is presented as the red line. A significant suppression of the strong OH background signal is observed, and a previously unresolved signal, located at radial distance ± 1 mm, is now clearly visible. A signal-to-noise ratio of approximately three is achieved for the single-shot measurements.

The spatial resolution in Fig. 3(b) is 2 mm in the vertical direction and 0.1 mm in the horizontal direction. The final resolution of the PFLIF image is set by the dimensions of the band-pass filter. These dimensions are, in turn, dictated by the spatial modulation frequency of the laser sheet and the spatial components of the object data. Theoretically, optimum spatial resolution is thus achieved by modulating the pump beam with a period of four pixels (half of the Nyquist frequency). In practice, however, imaging systems, particularly those based on intensified cameras, are often incapable of resolving such high spatial frequencies. For the current setup, the minimum number of pixels required to represent one modulation period is estimated to be 10 pixels (current value is 42). Improving the PFLIF system accordingly would boost the vertical spatial resolution by a factor of 8.

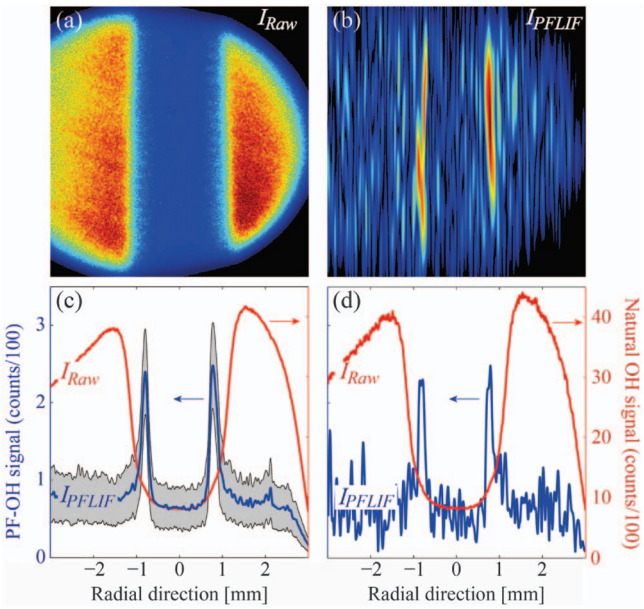

Fig. 3. (a) I_{RAW}, single-shot image collected with PFLIF having a modulated pump pulse in a CH_4/air flame. (b) I_{PFLIF}, extracted OH photofragment signal from I_{RAW}. (c) Red line, 2 mm vertical cross section of 300 single-shot images of I_{RAW}. The gray area shows the standard deviation from a 2 mm vertical cross section of 300 single-shot images of I_{PFLIF} and the thick blue line is the mean value of a 2 mm vertical cross section from these 300 single-shot images. (d) Red line, 2 mm vertical cross section of I_{RAW}; blue line, 2 mm vertical cross section of I_{PFLIF}.

The background in the final image has been suppressed about 50 times, which gives an increase in signal-to-interference ratio of about 20 for single-shot data by comparing the maximum background signal induced by the probe beam with the significantly weaker OH photofragment signal. Both the signal-to-noise and signal-to-interference ratio in stationary environments clearly show single-shot capabilities in nonstationary environments. However, a higher modulation frequency, as well as a larger band-pass filter, will provide more detailed structure and a higher spatial resolution in nonstationary environments. For imaging of OH photofragments stemming from HO_2 in turbulent flames, it is important to select an OH excitation line with minimal temperature sensitivity. In such an application, excitation via the $Q_1(5)$ transition, instead of the overlapping $Q_1(1)/R_2(3)$ line employed in the present demonstration, is preferable.

In summary, photofragmentation laser-induced fluorescence has for the first time, to the best of our knowledge, been combined with SI. By spatially modulating the pump pulse, a well-defined spatial frequency was given to the OH photofragments, making them easily recognized in the frequency domain. By using a post-processing routine based on spatial frequency lock-in detection, the OH-photofragment signal could be discriminated against the significantly stronger overlapping signal from naturally present OH radicals in the flame. This enables single-shot capabilities and shows an increase in signal-to-interference ratio of about 20 for this technique.

Funding. Energimyndigheten (Swedish Energy Agency) (CECOST 22538-3, CECOST 38913-1).

Acknowledgment. The authors would like to thank Igor Buzuk for technical support, as well as Tetra Pak Packaging Solutions for in-kind support.

REFERENCES

1. N. E. Henriksen and V. Engel, Int. Rev. Phys. Chem. **20**, 93 (2001).
2. M. Fushitani, Annu. Rep. Prog. Chem. Sect. C **104**, 272 (2008).
3. M. Nuss, D. Auston, and F. Capasso, Phys. Rev. Lett. **58**, 2355 (1987).
4. C. Lienau, J. C. Williamson, and A. H. Zewail, Chem. Phys. Lett. **213**, 289 (1993).
5. J. B. Simeonsson and R. C. Sausa, Appl. Spectrosc. Rev. **31**, 1 (1996).
6. J. B. Simeonsson and R. C. Sausa, TrAC Trends Anal. Chem. **17**, 542 (1998).
7. M. O. Rodgers, K. Asai, and D. D. Davis, Appl. Opt. **19**, 3597 (1980).
8. O. Johansson, J. Bood, M. Aldén, and U. Lindblad, Appl. Spectrosc. **62**, 66 (2008).
9. O. Johansson, J. Bood, B. Li, A. Ehn, Z. S. Li, Z. W. Sun, M. Jonsson, A. A. Konnov, and M. Aldén, Combust. Flame **158**, 1908 (2011).
10. M. A. A. Neil, R. Juškaitis, and T. Wilson, Opt. Lett **22**, 1905 (1997).
11. E. Berrocal, E. Kristensson, M. Richter, M. Linne, and M. Aldén, Opt. Express **16**, 17870 (2008).
12. E. Kristensson, A. Ehn, J. Bood, and M. Aldén, Proc. Combust. Inst. **35**, 3689 (2015).